PHYSICAL REVIEW C
NUCLEAR PHYSICS

THIRD SERIES, VOLUME 59, NUMBER 6 JUNE 1999

RAPID COMMUNICATIONS

The Rapid Communications section is intended for the accelerated publication of important new results. Manuscripts submitted to this section are given priority in handling in the editorial office and in production. A Rapid Communication in **Physical Review C** *may be no longer than five printed pages and must be accompanied by an abstract. Page proofs are sent to authors.*

Proton emission from the closed neutron shell nucleus ^{155}Ta

J. Uusitalo,[1] C. N. Davids,[1] P. J. Woods,[2] D. Seweryniak,[1,3] A. A. Sonzogni,[1] J. C. Batchelder,[4] C. R. Bingham,[5] T. Davinson,[2] J. deBoer,[6] D. J. Henderson,[1] H. J. Maier,[6] J. J. Ressler,[3] R. Slinger,[2] and W. B. Walters[3]
[1]*Physics Division, Argonne National Laboratory, Argonne, Illinois 60439*
[2]*University of Edinburgh, Edinburgh EH9 3JZ, United Kingdom*
[3]*Department of Chemistry, University of Maryland, College Park, Maryland 20742*
[4]*UNIRIB, Oak Ridge Associated Universities, Oak Ridge, Tennessee 37831*
[5]*Department of Physics and Astronomy, University of Tennessee, Knoxville, Tennessee 37996*
[6]*Sektion Physik, University of Munich, Am Coulombwall 1, D-85748 Garching, Germany*
(Received 2 March 1999)

Proton radioactivity from the closed neutron shell nucleus ^{155}Ta has been observed. It was produced via the *p4n* fusion evaporation channel using a ^{58}Ni beam on a ^{102}Pd target. The measured decay properties are $E_p = 1765(10)$ keV and $t_{1/2} = 12^{+4}_{-3}$ μs. Spin and parity $J^\pi = 11/2^-$ and a spectroscopic factor $S_p^{\rm exp} = 0.58^{+0.20}_{-0.15}$ characterize the decaying state.
[S0556-2813(99)50106-4]

PACS number(s): 23.50.+z, 21.10.Tg, 27.70.+q, 21.10.Dr

Many new examples of proton radioactivity have recently been discovered. This data was used to explore the evolution of nuclear structure and binding beyond the proton drip line, and to study proton transition rates [1]. In the present Rapid Communication, proton radioactivity is reported from the nucleus ^{155}Ta which has a magic neutron number ($N=82$) and is expected to be spherical in shape. Proton decay rates of spherical nuclei found in this region of the proton drip line have been accurately reproduced by WKB barrier-penetrability calculations combined with spectroscopic factors obtained from a low-seniority shell-model calculation [2]. The barrier-penetration probability is highly sensitive to the orbital angular momentum of the emitted proton; consequently, proton decay partial half-life measurements can be used to infer proton shell-model configurations in the parent nucleus. For a detailed understanding of the variation of proton transition rates from a given shell it is necessary to introduce a proton decay spectroscopic factor. In the $Z=64-82$ shell-model space, the low-seniority shell-model calculation assumes degenerate $2s_{1/2}$, $1d_{3/2,}$ and $0h_{11/2}$ proton orbitals with spectator neutrons. This model predicts proton spectroscopic factors, $S_p = P/9$, where P represents the number of proton hole pairs in the daughter nucleus compared to the $Z=82$ closed shell [2]. Subsequently, more sophisticated theoretical approaches have been applied to reproduce the spectroscopic factors [3].

Proton radioactivity was earlier observed from the more stable isotope ^{157}Ta, and it was assigned to a $s_{1/2}$ ground-state configuration [4]. The proton decay spectroscopic factor for this state of 0.56(24) agrees with the low-seniority shell-model prediction of 0.56 [2]. An alpha decaying state was identified in ^{157}Ta at an excitation energy of 22(5) keV and assigned to an $h_{11/2}$ isomer [4], the high orbital angular momentum suppressing the proton decay branch despite the higher available energy. In the intervening odd-odd isotope ^{156}Ta, ground and isomeric proton decaying states have been assigned to $[\pi d_{3/2} \nu f_{7/2}]^{2-}$ and $[\pi h_{11/2} \nu f_{7/2}]^{9+}$ configurations, respectively [5,6].

The proton-rich nucleus $^{155}_{73}$Ta$_{82}$ was produced via the *p4n* fusion evaporation channel using a ^{58}Ni beam from the ATLAS accelerator complex at Argonne National Laboratory to bombard a 1.0 mg/cm^2 thick, 78% enriched, ^{102}Pd target. Bombarding energies of 315 MeV and 320 MeV resulted in excitation energies of the compound nucleus of 77 MeV and 80 MeV, respectively, in the middle of the target with a range of ~ 10 MeV over the whole target thickness.

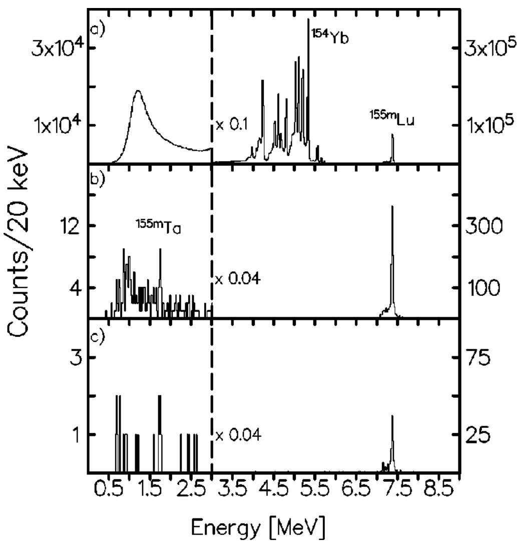

FIG. 1. (a) The total decay spectrum vetoed with the box detectors and with the back detector (see text for details). (b) The decay spectrum correlated with implants of mass $A=155$ and with maximum time between implant and decay of 30 μs. (c) Same as (b) but, in addition, a second decay was required as described in the text. In spectra (b) and (c) the vetoes are still in effect. Note the change in the scale at 3 MeV.

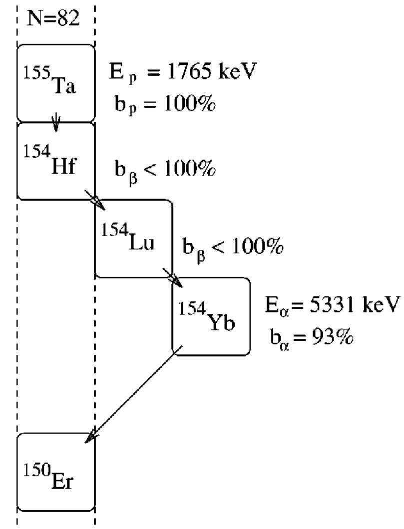

FIG. 2. The ^{155}Ta proton decay is followed by a decay chain with two slow β decays and an alpha decaying grandgrand daughter ^{154}Yb.

The total doses impinging on the target were 1.3×10^{15} particles and 1.7×10^{15} particles, respectively. The fragment mass analyzer (FMA) [7] was used to separate the reaction products from the beam, and to disperse them by mass and charge (A/Q). The FMA was set to focus mass $A=155$ and charge-state $Q=28$, with $Q=27$ and $Q=29$ collected at the same time. At the focal plane a position-sensitive parallel grid avalanche counter (PGAC) was installed to measure the A/Q of each ion. After passing through the focal plane detector, the reaction products were implanted into a double-sided silicon strip detector (DSSD), with thickness 65 μm, area 16×16 mm^2, and having 48 orthogonal strips on the front and rear [8]. This thickness of the DSSD is sufficient to stop 2 MeV protons and 8 MeV alpha particles, while positrons will cause only small signals which in most cases are below the electronic threshold. About 10% of the total *p4n* fusion evaporation yield was implanted in the DSSD. The time of arrival, position, and energy of the implants were recorded. This information was then correlated with the subsequent decays in the same position. In front of the DSSD were placed four silicon detectors, forming a six cm-deep box. These detectors were used as veto counters, helping to reduce the background caused mainly by escaping alphas in the energy region where possible discrete proton decay energies were expected. Behind the DSSD a large $(5\times5\,\mathrm{cm}^2)$ 500 μm thick silicon detector was placed. It was used to veto background events caused mainly by the transmission of high energy β-delayed protons. The proton decay energy calibration was performed using the known proton decay lines of ^{147}Tm, $E_p=1051(3)$ keV and ^{147m}Tm, $E_p=1119(5)$ keV [9], produced in a separate bombardment using the ^{58}Ni+^{92}Mo reaction.

Figure 1(a) shows the total decay spectrum observed in the DSSD, while Fig. 1(b) shows decay events correlated with mass $A=155$ implants within a maximum time interval of 30 μs between implant and decay. This spectrum is dominated by the short-lived alpha decay of the high-spin isomer in ^{155}Lu ($E=7390(5)$ keV, $t_{1/2}=2.71(3)$ ms [10]). Note that the relatively high energy of this alpha decay produces an escape bump (associated with particles not successfully vetoed by the auxiliary detectors) shifted to a lower energy compared to the corresponding feature in Fig 1(a). A small peak is present on the high energy tail of this escape bump at an energy of 1765(10) keV with a half-life $t_{1/2}=12^{+4}_{-3}$ μs. The ^{155m}Lu alpha decay peak was used to obtain a correction for the pileup effect caused by the fast decay energy signal falling on the tail of the implant signal. This effect was significant for decays faster than 20 μs. The probability that a fluctuation of the background distribution would produce the observed number of events in the small peak is less than 3×10^{-4}. This peak is too low in energy to be an alpha decay and must correspond to a proton decay. The most plausible $A=155$ candidate for proton decay is ^{155}Ta. ^{155}Hf is known to β decay, and being an even-Z nucleus, it is predicted to be strongly bound to proton emission [11]. ^{155}Lu has been thoroughly studied and only alpha decay transitions have been identified [10].

The proton decay of ^{155}Ta should be followed by two unobserved β decays and an alpha decay. The daughter ^{154}Hf β decays with a half-life of 2 s [12] to ^{154}Lu which in turn β decays with a half-life of 1.12 s [12] to the great granddaughter ^{154}Yb. ^{154}Yb has a 93% alpha branch ($E=5331(2)$ keV [13]), and it decays with a half-life of $t_{1/2}=0.41$ s [13]. This decay chain is illustrated in Fig. 2.

Figure 1(c) represents those decay events in Fig. 1(b) which are correlated with second-generation ^{154}Yb alpha decays within a maximum time interval of 15 s, while at the same time rejecting those cases where there was an $A=154$ implant in a 4 second time window preceding the alpha decay in the same detector position. This requirement rejects those cases where there was a real ^{154}Yb recoil (or ^{154}Lu recoil) implanted into the same pixel between the candidate for proton decay and the ^{154}Yb alpha decay. This is necessary because of the high production rate of ^{154}Yb alpha de-

TABLE I. Measured and calculated decay properties of ^{155}Ta.

Measured Q_p [keV]	Measured $t_{1/2}$ [μs]	WKB-$t_{1/2}$ [μs]	Proton orbital
		4.3×10^{-4}	$2s_{1/2}$
1776(10)	12^{+4}_{-3}	3.5×10^{-3}	$1d_{3/2}$
		7.0	$0h_{11/2}$

cays and the long correlation time difference between the proton and the alpha decays, due to the two intervening β decays. The expected number of remaining random correlations in the energy region of the small proton peak was calculated to be less than 2, based on the method given in Ref. [14], whereas a total of six correlations between ^{154}Yb alphas and the candidate ^{155}Ta protons were found. The probability, that the six observed correlations were produced by chance is less than 0.02. Hence, we conclude that the peak at 1765(10) keV in Fig. 1(b) does indeed correspond to the proton decay of ^{155}Ta.

The predicted partial β-decay half-life for ^{155}Ta$\sim$0.3 s [15], is long compared to the measured half-life of 12^{+4}_{-3} μs and, hence, a proton branching ratio $b_p = 1.00$ is assumed. From the measured proton decay yield, using the FMA efficiency of 10% and the above branching ratio the cross section for producing ^{155}Ta was deduced to be approximately 60 nb. This represents a reduction by a factor of 25 when compared to the yield obtained for ^{156}Ta [6] produced via the *p3n* fusion evaporation channel.

Table I shows the results of half-life calculations using the WKB barrier approximation with the real part taken from the Becchetti-Greenlees optical potential [16]. The measured half-life can only be explained by $l=5$ emission, corresponding to an $h_{11/2}$ configuration. From the ratio of theoretical and measured half-lives a spectroscopic factor $S_p^{\mathrm{exp}} = 0.58^{+0.20}_{-0.15}$ is obtained. This is in good agreement with the theoretical spectroscopic factor of $S_p^{\mathrm{th}} = 0.56$ predicted by the low-seniority shell model [2] and is consistent with the state being a very pure spherical shell-model configuration, as might be expected for an isolated state in a closed shell nucleus.

It is most likely that the proton decaying $h_{11/2}$ state is situated close in energy to the $s_{1/2}$ configuration as in the neighboring isotopes ^{157}Ta [4] and ^{159}Ta [2]. The ^{155}Ta $s_{1/2}$ state proton decay would be too short lived for detection in the present experiment and, furthermore, being a low-spin state, it would most likely have been produced with at least an order of magnitude smaller cross section than the high-spin state.

The proton decay Q value for the $h_{11/2}$ state in ^{155}Ta of 1776(10) keV compares with values of 954(14) and 438(12) keV [2] for the respective states in ^{157}Ta and ^{159}Ta. In general one expects the proton decay Q value to increase monotonically with decreasing neutron number for a given Z ignoring odd-even effects [17]. In this case, there is a significant decrease in proton binding for ^{155}Ta compared to the neighboring nuclei. One might therefore speculate that this effect is associated with the $N=82$ shell closure. If, however, one performs a similar analysis on Lu isotopes, there is no evidence for such an $N=82$ shell closure effect, although the proton in ^{153}Lu is significantly more bound than that in ^{155}Ta. It will be interesting to see if other cases of such behavior are found for other regions of the proton drip line.

In summary, proton emission from the closed neutron shell-nucleus ^{155}Ta has been identified. The measured decay rate is well reproduced assuming a spherical nucleus with an $h_{11/2}$ proton configuration. This represents an ideal test case for the theory of proton emission from spherical nuclei and provides further confidence in our detailed understanding of this phenomenon.

P.J.W. and T.D. wish to acknowledge travel support from NATO under Grant No. CRG 940303. This work was supported by the U.S. Department of Energy, Nuclear Physics Division, under Contract No. W-31-109-ENG-38.

[1] P.J. Woods and C.N. Davids, Annu. Rev. Nucl. Part. Sci. **47**, 541 (1997).
[2] C.N. Davids, P.J. Woods, J.C. Batchelder, C.R. Bingham, D.J. Blumenthal, L.T. Brown, B.C. Busse, L.F. Conticchio, T. Davinson, S.J. Freeman, D.J. Henderson, R.J. Irvine, R.D. Page, H.T. Penttilä, D. Seweryniak, K.S. Toth, W.B. Walters, and B.E. Zimmerman, Phys. Rev. C **55**, 2255 (1997).
[3] S. Åberg, P.B. Semmes, and W. Nazarewicz, Phys. Rev. C **56**, 1762 (1997); **58**, 3011 (1998).
[4] R.J. Irvine, C.N. Davids, P.J. Woods, D.J. Blumenthal, L.T. Brown, L.F. Conticchio, T. Davinson, D.J. Henderson, J.A. Mackenzie, H.T. Penttilä, D. Seweryniak, and W.B. Walters, Phys. Rev. C **55**, R1621 (1997).
[5] R.D. Page, P.J. Woods, R.A. Cunningham, T. Davinson, N.J. Davis, S. Hofmann, A.N. James, K. Livingston, P.J. Sellin, and A.C. Shotter, Phys. Rev. Lett. **68**, 1287 (1992).
[6] K. Livingston, P.J. Woods, T. Davinson, N.J. Davis, S. Hofmann, A.N. James, R.D. Page, P.J. Sellin, and A.C. Shotter, Phys. Rev. C **48**, R2151 (1993).
[7] C.N. Davids, B.B. Back, K. Bindra, D.J. Henderson, W. Kutschera, T. Lauritsen, Y. Nagame, P. Sugathan, A.V. Ramayya, and W.B. Walters, Nucl. Instrum. Methods Phys. Res. B **70**, 358 (1992).
[8] P.J. Sellin, P.J. Woods, D. Branford, T. Davinson, N.J. Davis, D.G. Ireland, K. Livingston, R.D. Page, A.C. Shotter, S. Hofmann, R.A. Hunt, A.N. James, M.A.C. Hotchkis, M.A. Freer, and S.L. Thomas, Nucl. Instrum. Methods Phys. Res. A **311**, 217 (1992).
[9] S. Hofmann, *Nuclear Decay Modes*, edited by D.N. Poenaru (IOP Publishing, Bristol, UK, 1996), p. 143.
[10] R.D. Page, P.J. Woods, R.A. Cunningham, T. Davinson, N.J. Davis, A.N. James, K. Livingston, P.J. Sellin, and A.C. Shotter, Phys. Rev. C **53**, 660 (1996).
[11] G. Audi and A.H. Wapstra, Nucl. Phys. **A565**, 66 (1993).
[12] R. B. Firestone, *Table of Isotopes*, 8th ed. (Wiley, New York, 1996), Vol. 2.

[13] A. Rytz, At. Data Nucl. Data Tables **47**, 205 (1991).

[14] K.-H. Schmidt, C.-C. Sahm, K. Pielenz, and H.-G. Clerc, Z. Phys. A **316**, 19 (1984).

[15] P. Möller, J.R. Nix, and K.-L. Kratz, At. Data Nucl. Data Tables **66**, 131 (1997).

[16] F.D. Becchetti and G.W. Greenlees, Phys. Rev. **182**, 1190 (1969).

[17] P.J. Woods, in *International School of Heavy Ion Physics, 4th Course: Exotic Nuclei*, edited by R.A. Broglia and P.G. Hansen (World Scientific, Singapore, 1998), p. 315.